Gold nanosphere enhanced green and red fluorescence in ZnO: Al, Eu3+

Swati Bishnoi, Rupali Das, and Santa Chawla

Citation: Applied Physics Letters **105**, 233108 (2014); doi: 10.1063/1.4904014

View online: http://dx.doi.org/10.1063/1.4904014

View Table of Contents: http://scitation.aip.org/content/aip/journal/apl/105/23?ver=pdfcov

Published by the AIP Publishing

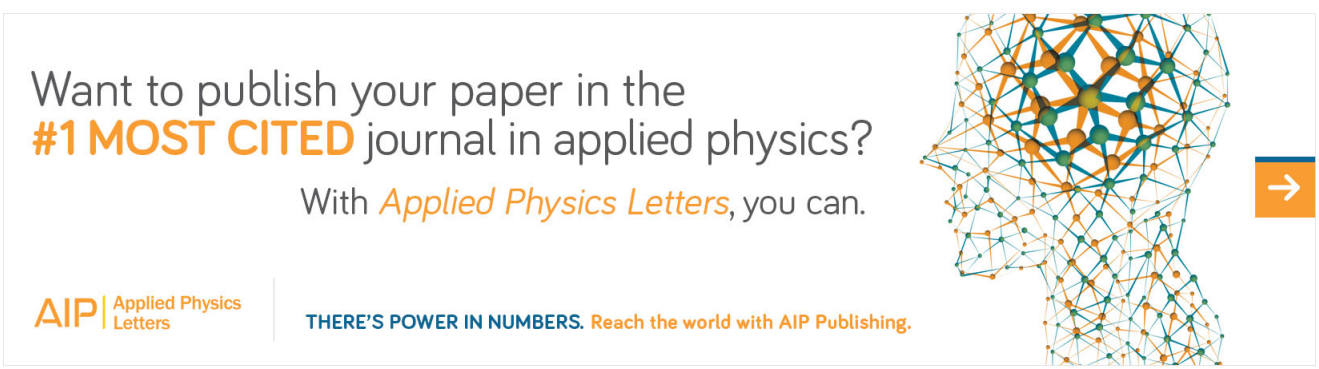

Gold nanosphere enhanced green and red fluorescence in ZnO: Al, Eu^{3+}

Swati Bishnoi, Rupali Das, and Santa Chawla[a)]
Luminescent Materials Group, CSIR-National Physical Laboratory, Dr. K. S. Krishnan Road, New Delhi-110012, India

(Received 10 November 2014; accepted 1 December 2014; published online 9 December 2014)

Gold nanoparticles can generate near field due to surface plasmon resonance (SPR) in the visible region. Such near field has the ability to enhance fluorescence of optimally proximal emitters. We have observed augmented green (intrinsic) and red (Eu^{3+}) emission under UV excitation (375 nm) from an important semiconductor ZnO:Al, Eu^{3+} when optimally conjugated with gold nanospheres. Local field generated by gold nanosphere (~30 nm) is simulated through finite difference time domain method, and a direct correlation with fluorescence enhancement is established. © *2014 AIP Publishing LLC*. [http://dx.doi.org/10.1063/1.4904014]

Zinc oxide, a direct band gap (~3.37 eV) multifunctional semiconductor, is an excellent emitter in the UV-visible region. Aluminum doped ZnO (AZO) shows good n-type conductivity[1,2] and offers low cost as compared to other transparent conducting oxides.[3] A luminescent AZO layer can be very effective in light emitting devices as well as photovoltaic applications. Doping AZO particles with light emitting lanthanide ions such as Eu^{3+} can make it an excellent fluorescence emitter.[4] Hence, by co doping Al and Eu^{3+} in ZnO host material, both fluorescent and electrical properties of ZnO can be enhanced. Though works have been reported on AZO[5,6] and Eu^{3+} doped ZnO[7,8] separately, report on fluorescence studies on Al and Eu^{3+} co doped ZnO is extremely rare.[9] Photoluminescence (PL) quenching of Rhodamine 6G dye due to fluorescence energy transfer to Au@ZnO core-shell nanoparticles[10] and enhancement and quenching of Eu^{3+} emission from Eu(III)EDTA,$3H_2O$ complex, in presence of Au@ZnO core-shell nanoparticles and Au nanoparticles,[11] indicate how proximity of emitter with metal nanoparticle can influence the recombination and energy transfer processes. Optimal conjugation of metal nanoparticles (MNP) with fluorescent particles is an effective way to augment fluorescence yield. Recently, surface plasmon resonance (SPR)-mediated tuning of emission property has been shown to be an effective way to improve the band emission of ZnO nanostructures,[12] localized Surface Plasmon Resonance (LSPR) enhanced emission in Au-decorated ZnO nanorod arrays have also been reported.[13] But, plasmonic enhancement of both intrinsic and rare earth emission in ZnO have been rarely explored, and we report enhancement of both green (intrinsic) and red (Eu^{3+}) emissions from Al and Eu^{3+} co doped ZnO due to proximity with Au nanoparticles.

The excitation of LSPR in metal nanoparticles results in the confinement of EM field in the nanoscale region very close to the metal surface and a considerable enhancement in the local density of optical states.[14,15] When a fluorescent nanoparticle is placed in proximity of such a metal nanoparticle, emission can be greatly enhanced through two possible mechanisms. One is the surface plasmon induced absorption enhancement of emitters due to the enhancement of the local electric field at the metal nanostructure interface, thus leading to fluorescence increment[16] by excitation enhancement. Another mechanism is the surface Plasmon coupled emission (SPCE)[17] which is achieved by coupling of emission energies with SP modes, or in simple words, spectral overlap of plasmon absorption band of MNP with emission band resulting in emission enhancement. Such fluorescence enhancement can be achieved by placing MNP's in close proximity to the phosphors particles; however, a thin dielectric spacer layer is required to prevent the undesirable quenching phenomenon[18] since non radiative energy transfer may occur when the fluorophore and MNP's are in direct contact.

ZnO:Al, Eu^{3+} was synthesized by controlled solid state diffusion process and showed hexagonal phase.[30] Gold (Au) nanoparticles were synthesized by colloid chemistry by optimizing the method developed by Turkevish[30] and TEM reveal formation of Au nanospheres[30] of average diameter 30 nm. The studied Au NP−ZnO:Al,Eu^{3+} integrated material system comprise of a thin film of ZnO:Al,Eu^{3+} particles and a layer of Au nanospheres separated by a thin spacer layer of polyvinyl alcohol (PVA) to avoid direct contact of both the species.[19] First ZnO:Al,Eu^{3+} particles were dispersed in a 3% solution of PVA in distilled water and coated on a microscope cover slip and dried. Over this layer, a pure PVA layer (3%) was deposited followed by a layer of Au nanoparticle by drop casting the colloidal solution of Au NPs. The graphical representation of the integrated thin film is presented in Fig. 1(a), the TEM images of Au NPs and ZnO:Al,Eu^{3+} particles are shown in the inset. The integrated material system is studied by confocal fluorescence imaging and spectroscopy. The sample was excited by 375 nm UV laser (10mW), matching the band gap energy of ZnO so that the effect of enhanced EM fields generated in the near field of Au nanospheres on the intrinsic emission of ZnO as well as the signature emission from the rare earth dopant Eu^{3+} can be investigated. The confocal fluorescence spectra are shown in Fig. 1(b) for samples corresponding to the confocal fluorescence scans Figs. 1(c) and 1(d), respectively, of ZnO:Al,Eu^{3+} phosphor and ZnO:Al:Eu^{3+}–Au NPs hybrid system. Integrated spectrum taken for ZnO:Al,Eu^{3+} and ZnO:Al,Eu^{3+}–Au NPs hybrid system reveal enhancement in fluorescence intensity in both

a)Author to whom correspondence should be addressed. Electronic mail: santa@nplindia.org

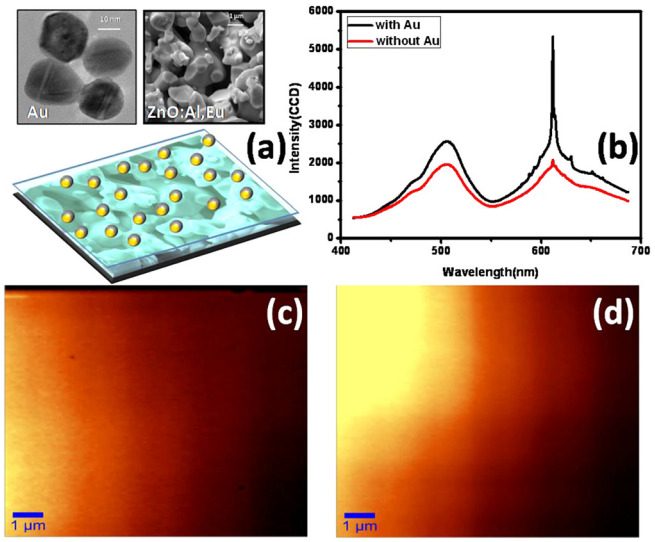

FIG. 1. (a) Graphical representation of arrangements of ZnO:Al,Eu NPs (sea green layer), PVA layer (transparent layer), and Au NPs (golden spheres) used for confocal fluorescence study, inset shows the TEM image of Au NPs and SEM image of ZnO:Al,Eu particles; (b) confocal fluorescence spectra (integrated) under 375 nm laser excitation; confocal fluorescence image of (c) ZnO:Al,Eu and (d) ZnO:Al,Eu+Au NP.

green and red region with signature Eu^{3+} emission peak at 611 nm ($^5D_0$–$^7F_2$ electric dipole transition) becoming prominent in the Au NP integrated sample. The enhancement is 133% for intrinsic green emission and 258% for Eu^{3+} red emission. The confocal fluorescence images (Figs. 1(c) and 1(d)) clearly show regions of bright fluorescence as well as considerable enhancement in the fluorescence intensity. To further enumerate the effect of plasmonic near field of exact Au nanospheres on fluorescence enhancement, we have done three dimensional finite difference time domain simulations (FDTD) to effectively calculate the EM field generated around Au NP. For simulation of LSPR properties of gold NPs, one representative Au NP image is taken from the TEM micrographs on the basis of average distribution of synthesized Au NPs. FDTD method has been widely used and is an effectual method for simulation of MNP[20–22] where solution of Maxwell's equations are obtained in both E (t) and H (t) by making them discrete in time to generate the steady state continuous wave field E (ω).

FDTD solutions (version 8.7.1)[23] have been used with mesh size 0.5 nm for spacing around the nanosphere taking conformal variant 1 condition. The E-field intensities were independent for the considered mesh size in x, y and z directions. The optical dielectric function of gold is modeled using the Johnson and Christy dispersion model.[24,30] The background refractive index was considered as 1.33 for water. A cubic Yee cell was considered with perfectly matched layer (PML) boundaries. Single particle absorption, scattering and extinction spectra have also been simulated using FDTD method (Fig. 2(b)), showing a dominant absorption peak at 511 nm. Since the size of Au NP is small, absorption is predominant and scattering is negligible resulting in predominance of absorption in the extinction process.[25] Measured UV-Visible absorption spectra of Au NP colloidal solution (shown in the inset) reveal broad dipolar peak centered at 528 nm (Fig. 2(a)) due to inhomogeneous damping caused by different spatial positions and random orientations of Au NPs of varied shapes in colloidal solution. Dipole LSPRs are excited efficiently by plane wave; they are known as bright modes; and they are broad as they suffer strong radiative damping. FDTD method was employed to calculate the generated EM field for the Au nanosphere at excitation wavelength 375 nm (Fig. 3(a)), LSPR frequency 528 nm (Fig. 3(b)), and emission wavelengths 505 nm (Fig. 3(c)) and 611 nm (Fig. 3(d)).

The simulated images clearly show strong dipolar field leading to significant localization of electric field in the near-field region. The calculated local electric field values reveal largest $|E|^2$ value at the dipolar LSPR frequency. At 375 nm excitation wavelength, the calculated $|E|^2$ value for the Au nanosphere is 16 times, and at LSPR, it is 29 times that of the incident field. The $|E|^2$ values indicate smaller field enhancement at emission wavelengths, e.g., 505 nm (intrinsic green emission from ZnO) and 611 nm (corresponding to red emission from Eu^{3+}) as can be easily discerned from FDTD simulated images (Figs. 3(c) and 3(d)).

Fluorescence enhancement due to LSPR of Au NPs can occur due to two factors mainly confinement and concentration of EM field into sub wavelength region (evaluated at the excitation frequency) and the increase in quantum yield which is connected to the modification of photonic density of states[26] (evaluated at the emission frequency) in the vicinity of the phosphor particle. However, the contributions of these two components cannot be distinguished very efficiently, particularly when broad LSPR band of Au NPs (Fig. 2(a)) overlap with both excitation and emission spectrum of the ZnO:Al,Eu^{3+} particles. Of the two mechanisms through which metal enhanced fluorescence (MEF) can occur, excitation enhancement (enhancement of local EM Field) produces a higher excitation rate but does not change the decay time of

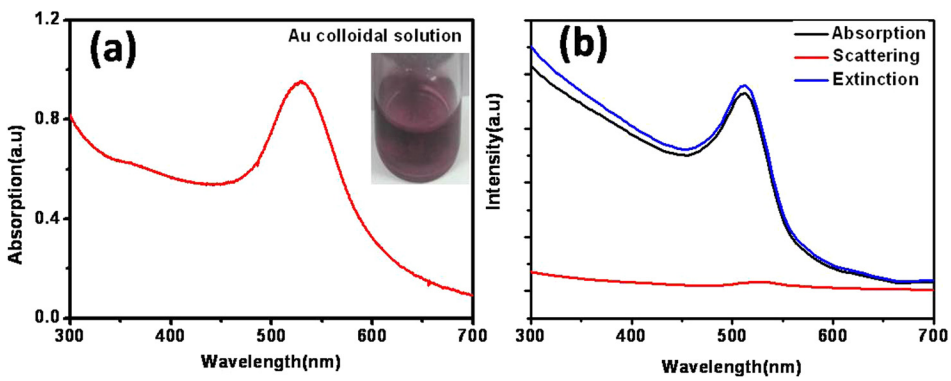

FIG. 2. (a) Measured UV-Visible absorption spectra of Au NP colloidal solution. The inset shows red coloured Au colloidal solution (b) simulated absorption, scattering, and extinction spectra of exact Au nanosphere, imported from TEM, using FDTD simulations.

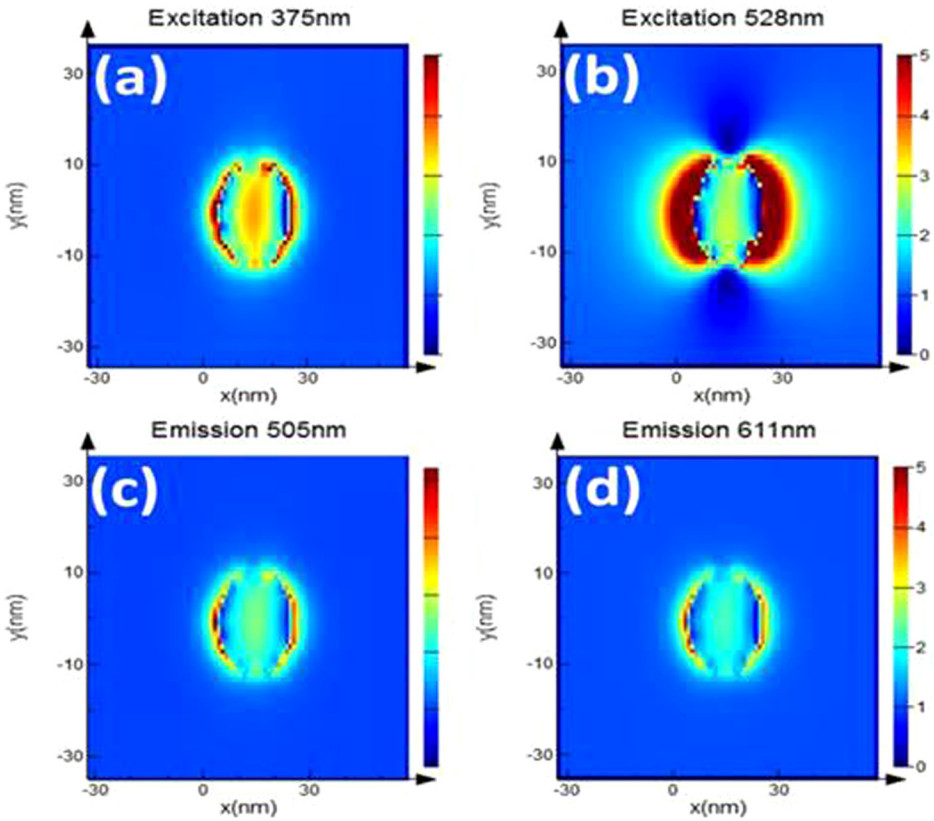

FIG. 3. Near field ($|E|^2$) image of Au nanosphere by FDTD simulation by importing exact TEM images of Au NP at different incident optical field energy (a) at excitation wavelength 375 nm, (b) at LSPR wavelength 528 nm, (c) ZnO emission wavelength 505 nm, and (d) Eu^{3+} emission wavelength 611 nm.

the fluorophore and emission enhancement increases the radiative decay rate thus reducing the luminescence decay time.[27] The fluorescence emission rate γ_{em} can be related to the excitation rate γ_{exc} and the total decay rate $\gamma = \gamma_r + \gamma_{nr}$ through the equation[28] $\gamma_{em} = \gamma_{exc}\,(\gamma_r/\gamma)$, where γ_r is the radiative decay rate and γ_{nr} is the non radiative decay rate. The emission probability (γ_r/γ) is also called the quantum yield of the emission process. Hence, in case of fluorescence enhancement (increase in quantum yield) by emission enhancement process, the radiative decay rate γ_r increases.

In our case, when Au NPs are conjugated with ZnO:Al,Eu^{3+} particles, we have measured the time resolved luminescence decay under 375 nm excitation of intrinsic ZnO green emission at 505 nm and $^5D_0$-$^7F_2$ red emission of Eu^{3+} at 611 nm as shown in Figs. 4(a) and 4(b), respectively. The decay could be fitted into a bi-exponential equation as given below

$$Fit = a + b_1 \cdot e^{-\frac{t}{\tau_1}} + b_2 \cdot e^{-\frac{t}{\tau_2}}.$$

The decay curve fittings and results of their detail analysis are listed in Table I which indicate that decay characteristics for green emission remain almost similar with and without Au NPs with a slight change in average decay time. This suggests that prominent mechanism for green emission enhancement would be through enhancement of near field due to presence of Au NPs in proximity. On the other hand, for red emission, average decay time (Table I) decreases from 1.02 μs to 0.94 μs after Au NP conjugation. The decrease in decay time is due to change in Eu^{3+} environment and the energy transfer from Au NP to Eu^{3+} $^5D_1$ level followed by phonon relaxation (non-radiative) to the emitting $^5D_0$ level leading to radiative transition to lower $^7F_2$ level causing fluorescence enhancement for Eu^{3+} red emission.

The ZnO:Al,Eu^{3+} nanophosphor under 375 nm excitation emits in the green region with a broad peak centered at 505 nm arising from the intrinsic point defects of ZnO and a sharp peak at 611 nm due to transitions between f-f levels ($^5D_0$-$^7F_2$) of Eu^{3+}. However, the corresponding integrated emission spectra (Fig. 1(b)) of ZnO:Al,Eu^{3+} in propinquity with Au NPs clearly elucidate enhancements in green fluorescence upto 133% and red emission up to 258% as compared to that of only ZnO:Al,Eu^{3+} under UV excitation. Green emission in ZnO under direct band edge excitation occurs when excited conduction band electrons relax to metastable donor state followed by radiative recombination with holes in the acceptor centre as shown in the energy level diagram (Fig. 4(c)). The mechanism for green emission remains same when conjugated with Au NPs, but local field enhancement produces a higher excitation rate and fluorescence is enhanced. The significant fluorescence enhancements could be attributed to the enhanced EM field of the Au NPs increasing excitation rate of bound excitons of ZnO. The Au NPs aptly localize the impinging EM field as near field around them, contributing towards the fluorescent enhancements. The energy level diagram also shows the energy level equivalent to the dipolar field generated around Au NP and energy transfer to ZnO and also direct coupling between the LSPR and the excited state[29] of Eu^{3+}. For red emission, there is energy transfer from Au NP to Eu^{3+} ion resulting in population of upper levels $^5D_1$ of Eu^{3+},[19] nonradiative (NR) energy transfer to lowest emitting state $^5D_0$ and characteristic red emission due to transition to the ^7F_J levels.

In summary, we have presented a comprehensive work involving chemical synthesis of spherical gold nanoparticles, Al and rare earth Eu^{3+} codoped ZnO, conjugation of Au NP and doped ZnO particles in a suitable hybrid structure that

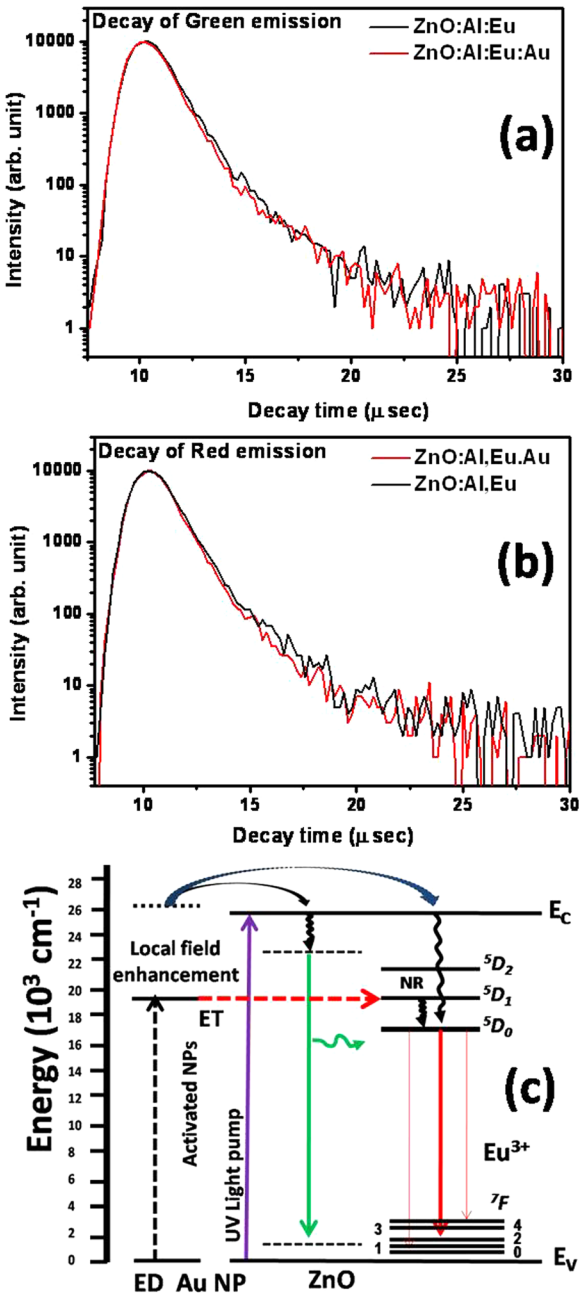

FIG. 4. Luminescence decay curves (a) for 505 nm green emission; (b) 611 nm red emission of ZnO:Al,Eu^{3+} with and without Au NPs; (c) energy level diagram showing scheme of excitation and emission process involving direct excitation across ZnO band gap, green emission from intrinsic point defects and energy transfer through EM field of Au NPs (black and red dotted arrows) to ZnO & Eu^{3+}, respectively, leading to fluorescence enhancement.

lead to about 258% fluorescence enhancement of red emission. We have used confocal fluorescence microscopy to irrefutably establish the fluorescence enhancement from doped ZnO:Al,Eu^{3+} particles in proximity of Au NPs due to LSPR coupling under excitation of UV light. For further supporting the experimental results, we have used FDTD simulation technique for estimating the near field generation by Au nanospheres, so as to understand the complete phenomenon of fluorescence enhancement supported by experimental and simulated results. Plasmon enhanced green and red emission under UV excitation have significant applications in solar cell and nano biotechnology.

TABLE I. Luminescence decay parameters.

Sample	τ_1 (μs) (Rel. %)	τ_2 (μs) (Rel. %)	$\tau_{av} = \frac{b_1\cdot\tau_1^2+b_2\cdot\tau_2^2}{b_1\cdot\tau_1+b_2\cdot\tau_2}$ (μs)
ZnO:Al:Eu [Ex-375 nm,Em-505 nm]	0.84 (99.61%)	7.25 (0.39%)	0.86
ZnO:Al:Eu-Au [Ex-375 nm,Em-505 nm]	0.80 (99.62%)	6.96 (0.38%)	0.82
ZnO:Al:Eu [Ex-375 nm,Em-611 nm]	0.95 (98.67%)	6.49 (1.33%)	1.02
ZnO:Al:Eu-Au [Ex-375 nm,Em-611 nm]	0.89 (91.64%)	4.80 (8.81%)	0.94

Authors acknowledge the research Grant under CSIR Solar mission TAPSUN programme.

[1]Z. Y. Ning, S. H. Cheng, S. B. Ge, Y. Chao, Z. Q. Gang, Y. X. Zhang, and Z. Liu, Thin Sol Films **307**, 50–53 (1997).
[2]K. Postava, H. Sueki, M. Aoyama, T. Yamaguchi, K. Murakami, and Y. Igasaki, Appl. Surf. Sci. **175/176**, 543–548 (2001).
[3]T. Minami, Semicond. Sci. Technol. **20**, S35–S44 (2005).
[4]A. Bril and W. L. Wanmaker, Philips Tech. Rev. **27**, 22 (1966).
[5]O. Lupan, S. Shishiyanu, V. Ursaki, H. Khallaf, L. Chow, T. Shishiyanu, V. Sontea, E. Monaico, and S. Railean, Sol. Energy Mater. Sol. Cells **93**, 1417–1422 (2009).
[6]Z. Lu, J. Zhou, A. Wang, N. Wangab, and X. Yang, J. Mater. Chem. **21**, 4161 (2011).
[7]T. S. Barros, B. S. Barros, S. Alves, Jr., R. H. A. G. Kiminami, H. L. Lira, and A. C. F. M. Costa, Mater. Sci. Forum **591–593**, 745–749 (2008).
[8]D. Wang, G. Xing, M. Gao, L. Yang, J. Yang, and T. Wu, J. Phys. Chem. C **115**, 22729–22735 (2011).
[9]Z. Wu, Y. Wang, J. Zhang, and Y. Wang, Integr. Ferroelectr. **146**, 161–167 (2013).
[10]K. K. Haldar, T. Sen, and A. Patra, J. Phys. Chem. C **112**, 11650–11656 (2008).
[11]K. K. Haldar and A. Patra, Appl. Phys. Lett. **95**, 063103 (2009).
[12]S. T. Kochuveedu, J. H. Oh, Y. R. Do, and D. H. Kim, Chem. Eur. J. **18**, 7467–7472 (2012).
[13]Y. Lin, C. Xu, J. Li, G. Zhu, X. Xu, J. Dai, and B. Wang, Adv. Optical Mater. **1**, 940–945 (2013).
[14]O. J. F. Martin, C. Girard, and A. Dereux, Phys. Rev. Lett. **74**, 526–529 (1995).
[15]U. Hohenester, H. Ditlbacher, and J. R. Krenn, Phys. Rev. Lett. **103**, 106801 (2009).
[16]A. M. Stefan, *Plasmonics: Fundamentals and Applications* (Springer, Berlin/Heidelberg, 2006).
[17]J. R. Lakowicz, Anal. Biochem. **324**, 153 (2004).
[18]W. Feng, L. D. Sun, and C. H. Yan, Chem. Commun. **29**, 4393–4395 (2009).
[19]P. Anger, P. Bharadwaj, and L. Novotny, "Enhancement and quenching of single-molecule fluorescence," Phys. Rev. Lett. **96**(11), 113002 (2006).
[20]A. Taflove and S. C. Hagness, *Computational Electrodynamics: The Finite-Difference Time-Domain Method* (Artech House, 2000).
[21]Z. Buch, V. Kumar, H. Mamgain, and S. Chawla, Chem. Commun. **49**, 9485 (2013).
[22]Z. Buch, V. Kumar, H. Mamgain, and S. Chawla, J. Phys. Chem. Lett. **4**, 3834 (2013).
[23]Reference Guide for FDTD Solutions, available at www.lumerical.com/fdtd.
[24]P. B. Jhonson and R. W. Christy, Phys. Rev. B **6**, 4370 (1972).
[25]D. D. Evanoff, Jr. and G. Chumanov, ChemPhysChem **6**, 1221 (2005).
[26]V. Giannini, A. I. F. Dominguez, and S. Maier, Small **6**, 2498 (2010).
[27]W. Deng, L. Sudheendra, J. K. Zhao, J. Fu, D. Jin, I. M. Kennedy, and E. M. Goldys, Nanotechnology **22**, 325604 (2011).
[28]S. A. Maier, *Plasmonics: Fundamentals and Applications* (Springer, Berlin/Heidelberg, 2007).
[29]V. A. G. Rivera, F. A. Ferri, and E. Marega, Jr., *Plasmonics—Principles and Applications* (Intech, 2012).
[30]See supplementary material at http://dx.doi.org/10.1063/1.4904014 for synthesis of Au NPs, synthesis of ZnO:Al,Eu phosphor, instrument detail, structure and morphology, and FDTD simulation parameters.